Open Access Research Journal of
Engineering and Technology
Journals home page: https://oarjpublication/journals/oarjet/
ISSN: 2783-0128 (Online)

OARJ OPEN ACCESS RESEARCH JOURNALS

(RESEARCH ARTICLE)

Nitric acid-treated *Luffa cylindrica* seeds as a sustainable biosorbent: Characterization and fixed-bed column performance for simultaneous removal of Ni (II), Cu (II), and Zn (II) from aqueous solutions

Diagbonya Paul [1,*], Dagde Kenneth Kekpugile [1] and Innocent Oseribho Oboh [2]

[1] *Department of Chemical/Petrochemical Engineering, Rivers State University, Nigeria.*
[2] *Department of Chemical Engineerng University of Uyo, Uyo, Nigeria.*

Open Access Research Journal of Engineering and Technology, 2026, 11(01), 001–014

Publication history: Received on 03 June 2026; revised on 12 July 2026; accepted on 15 July 2026

Article DOI: https://doi.org/10.53022/oarjet.2026.11.1.0052

Abstract

The escalating contamination of water resources by toxic heavy metals demands the development of cost-effective and sustainable remediation technologies. This study investigated the application of nitric acid-treated *Luffa cylindrica* (LC) seeds as a novel biosorbent for the simultaneous removal of Ni(II), Cu(II), and Zn(II) ions from aqueous solutions using a continuous fixed-bed column system. The LC adsorbent was produced at a carbonation temperature of 105 degrees C and comprehensively characterized using Fourier Transform Infrared (FTIR) spectroscopy, Scanning Electron Microscopy (SEM), and Brunauer-Emmett-Teller (BET) analysis. The BET surface area, pore volume, pore diameter, and bulk density were determined as 23.971 m squared/g, 0.011 cc/g, 2.402 nm, and 0.34 g/cm cubed, respectively. FTIR analysis identified hydroxyl, carboxyl, and carbonyl functional groups as active binding sites for metal chelation. The effects of column bed height (5, 7.5, 10 cm), injection flow rate (5, 10, 15 mL/min), and initial metal concentration (10, 20, 30 g/L) on adsorption performance were systematically evaluated. Results demonstrated that increasing bed height significantly enhanced metal removal efficiency, achieving maximum removals of 83.07% for Ni(II), 51.66% for Cu(II), and 55.73% for Zn(II) at 10 cm bed height with 5 mL/min flow rate. Conversely, elevated flow rates and larger adsorbent particle sizes (above 75 micrometer) reduced removal efficiency due to decreased residence time and increased diffusion resistance. The optimal operating conditions were established as 10 cm bed height, 5 mL/min flow rate, and 75 micrometer particle size. The pseudo-second-order kinetic model provided the best fit (R squared = 1.000), indicating chemisorption as the rate-controlling mechanism. This study establishes LC seeds as a promising, eco-friendly, and economically viable biosorbent for heavy metal remediation in wastewater treatment applications.

Keywords: *Luffa cylindrica*; Biosorption; Heavy metals; Fixed-bed column; Characterization; Nickel; Copper; Zinc; Wastewater treatment

1. Introduction

The rapid industrialization and urbanization witnessed globally over the past decades have precipitated an unprecedented escalation in environmental pollution, particularly the contamination of aquatic ecosystems by toxic heavy metals (Babel & Kurniawan, 2003; Gupta *et al*., 2009). Industrial effluents from metal plating, mining operations, electrical manufacturing, and agricultural runoff containing fertilizers and fungicidal sprays constitute primary sources of heavy metal pollution in surface and groundwater resources (Abdel-Ghani *et al*., 2009). The metals of most immediate environmental concern include cadmium, chromium, cobalt, copper, nickel, mercury, and zinc, owing to their non-biodegradable nature, bio-accumulative tendencies, and deleterious health effects on humans and ecosystems even at trace concentrations (WHO, 2017; Wosu, 2024; Wosu & Ekokoye, 2025).

Among these pollutants, nickel, copper, and zinc represent particularly significant concerns due to their widespread industrial applications and substantial presence in wastewater discharges. Nickel contamination arises from

*Corresponding author: Diagbonya Paul

electroplating, battery manufacturing, and mining activities, causing dermatitis, respiratory disorders, and carcinogenic effects upon prolonged exposure (Singh, 2008). Copper, extensively utilized in electrical wiring, metal plating, and agricultural chemicals, induces gastrointestinal distress, liver damage, and Wilson's disease at elevated concentrations (Tumin *et al*., 2008). Zinc, though an essential micronutrient, becomes toxic at concentrations exceeding 100-500 mg/day, with industrial sources including galvanizing plants, acid mine drainage, and municipal wastewater treatment facilities (Rakesh *et al*., 2010). The World Health Organization has established maximum acceptable concentrations of 0.02 mg/L for nickel, 2.0 mg/L for copper, and 5.0 mg/L for zinc in drinking water, emphasizing the critical need for effective remediation technologies (WHO, 2017).

Conventional physicochemical treatment technologies for heavy metal removal encompass coagulation-flocculation, chemical precipitation, ion exchange, membrane filtration, electrochemical treatment, and reverse osmosis (Ariffin *et al*., 2017). Despite demonstrating reasonable removal efficiencies, these methods are frequently associated with significant limitations including high operational costs, excessive chemical sludge generation, incomplete metal removal at low concentrations, high energy consumption, and potential secondary pollution (Gupta & Ali, 2013). These drawbacks have catalyzed intensive research toward the development of alternative, cost-effective, and environmentally sustainable treatment approaches.

Adsorption has emerged as one of the most promising techniques for heavy metal remediation due to its operational simplicity, high efficiency, cost-effectiveness, and applicability across wide concentration ranges (Dabrowski, 2001; Ojong *et al*., 2025; Ojong &Wosu, 2025). Activated carbon, the most widely employed adsorbent, exhibits exceptional removal capacities for diverse contaminants; however, its high production and regeneration costs constrain large-scale deployment, particularly in developing economies (Babel and Kurniawan, 2003; Okezua *et al*., 2025). This economic barrier has stimulated considerable interest in the identification and development of low-cost, locally available alternative adsorbents derived from agricultural wastes and biomass residues.

Biosorption, defined as the passive uptake of metal ions by biological materials through various physicochemical mechanisms, represents a particularly attractive alternative (Volesky, 2003). The process offers numerous advantages including low cost, minimal sludge generation, high metal binding capacity, potential for metal recovery, and applicability across diverse environmental conditions. Various biosorbents have been investigated, including microbial biomass, agricultural residues, and plant materials such as peat, lignite, peanut hulls, coconut coir, and sugarcane bagasse (Richard, 2009). The lignocellulosic composition of plant materials, comprising cellulose, hemicellulose, pectin, and lignin, provides abundant functional groups including hydroxyl, carboxyl, and carbonyl moieties that serve as active binding sites for metal chelation and ion exchange (Volesky, 2003).

Luffa cylindrica (L.) Roem., commonly known as sponge gourd or loofah, belonging to the family Cucurbitaceae, represents a particularly promising candidate for biosorption applications. This tropical and subtropical climbing vine is extensively cultivated across West Africa, Asia, and South America for its fibrous fruit network, traditionally utilized as natural sponges (Mazali& Alves, 2005). The seeds, often discarded as agricultural waste during fiber extraction, contain substantial quantities of lignocellulosic material with abundant surface functional groups. Previous studies have demonstrated the effectiveness of L. cylindrica fibers for dye removal (Segun *et al*., 2014), chromium(VI) adsorption (Moreno-Rubio *et al*., 2025; Laidani*et al*., 2020), and heavy metal uptake (Nwosu-Obieogu *et al*., 2020; Sasan *etal*., 2023). However, comprehensive investigations focusing specifically on L. cylindrica seeds for simultaneous multi-metal removal in continuous column systems remain notably scarce in the literature.

Fixed-bed column systems offer significant advantages over batch configurations for practical wastewater treatment applications, including continuous operation, higher treatment capacities, simpler scaling procedures, and greater process automation potential (Himanshu, 2019). The dynamic behavior of adsorption columns is influenced by multiple operational parameters including bed height, influent flow rate, initial contaminant concentration, and adsorbent particle size, all of which require systematic optimization to maximize removal efficiency and minimize operational costs.

Despite the growing body of research on L. cylindrica-based adsorbents, several critical knowledge gaps persist: (i) limited characterization of nitric acid-treated L. cylindrica seeds specifically for multi-metal systems; (ii) insufficient understanding of the combined effects of bed height, flow rate, and particle size on simultaneous Ni(II), Cu(II), and Zn(II) removal; (iii) inadequate mechanistic interpretation of adsorption dynamics in continuous column configurations; and (iv) the need for comparative performance evaluation against established biosorbents. This study was designed to systematically address these gaps through comprehensive characterization and parametric optimization of a fixed-bed column system utilizing nitric acid-treated L. cylindrica seed biosorbent.

The justification for this research derives from the urgent need for affordable, locally sourced, and environmentally benign adsorbents capable of simultaneous multi-metal removal from complex industrial wastewaters. The utilization of L. cylindrica seeds, an abundant agricultural byproduct in Nigeria and other tropical regions, aligns with circular economy principles while addressing critical water quality challenges. The specific objectives were to: (1) produce and characterize nitric acid-treated L. cylindrica seed adsorbent using FTIR, SEM, and BET analytical techniques; (2) evaluate the effects of bed height, injection flow rate, and adsorbent particle size on the simultaneous removal of Ni(II), Cu(II), and Zn(II) ions; (3) assess the influence of operational parameters on effluent physicochemical properties including pH, TDS, DO, COD, and BOD; and (4) determine optimal operating conditions for maximum metal removal efficiency.

2. Materials and methods

2.1. Materials

The *Luffa cylindrica* seeds utilized in this research were collected from mature, sun-dried L. cylindrica fruits obtained from local farms in Port Harcourt, Rivers State, Nigeria. The seeds were stored in clean polyethylene bags and transported to the laboratory for processing. Analytical grade chemicals including Copper(II) tetraoxosulphate(VI) pentahydrate (CuSO4.5H2O), Zinc(II) chloride (ZnCl2), and Nickel(II) tetraoxosulphate(VI) hexahydrate (NiSO4.6H2O) were purchased from BDH Chemicals Ltd (Poole, England). Concentrated nitric acid (HNO3, 65%) for adsorbent digestion was obtained from Sigma-Aldrich (St. Louis, USA). Glass wool, glass beads (5 mm diameter), and all other laboratory reagents were of analytical grade and used without further purification. Stock solutions of individual metal ions were prepared by dissolving precise quantities of the respective metal salts in deionized water and diluting to standard concentrations.

2.2. Preparation of *Luffa cylindrica* Seed Adsorbent

The collected L. cylindrica seeds were thoroughly washed with deionized water to remove surface contaminants, dust, and adhering pulp residues. The cleaned seeds were subsequently dried in a hot air oven (Model WT34LOV-S, Ravinder Sinh) at 105 degrees C for 24 hours to achieve constant weight and prevent microbial degradation. The dried seeds were ground using a laboratory grinding mill (Christy Lab Mill, Christy Turner Ltd., England) and sieved through standard ASTM test sieves to obtain uniform particle sizes of 75 micrometer, 150 micrometer, and 300 micrometer for parametric studies. The ground biosorbent was chemically activated by digestion in 0.1 M nitric acid solution at a solid-to-liquid ratio of 1:10 (w/v) for 2 hours at ambient temperature (29 plus or minus 2 degrees C) with continuous stirring at 200 rpm using a magnetic stirrer. The acid treatment served to protonate surface functional groups, enhance porosity, and increase the density of active binding sites (Adeyinka *et al*., 2007). Following digestion, the biosorbent was filtered through Whatman No. 1 filter paper, repeatedly washed with deionized water until neutral pH was attained, and oven-dried at 105 degrees C for 12 hours. The processed adsorbent was stored in airtight containers for subsequent characterization and adsorption experiments.

2.3. Characterization of Biosorbent

The surface functional groups of the raw and metal-loaded L. cylindrica seed biosorbent were identified using Fourier Transform Infrared (FTIR) spectroscopy (Cary 630, Agilent Technologies) employing the potassium bromide (KBr) pellet technique. Approximately 0.1 g of biosorbent was mixed with 0.25-0.50 g of spectroscopic-grade KBr and compressed into transparent pellets under vacuum. The spectra were recorded in the wavenumber range of 350-4000 cm-1 with a resolution of 4 cm-1 and 32 scans per sample. The morphological characteristics and surface topography were examined using Phenom Prox Scanning Electron Microscope (SEM) at accelerating voltages of 5-15 kV. Biosorbent samples were mounted on aluminum stubs using conductive adhesive tape, gold-coated under vacuum to enhance conductivity, and examined at magnifications of 500x, 1000x, and 2000x. The Brunauer-Emmett-Teller (BET) surface area, pore volume, and pore size distribution were determined using QuantachromeNovaWin Instrument (version 11.03) via nitrogen adsorption-desorption isotherms at 77 K. Prior to analysis, approximately 1 g of sample was degassed at 523.15 K under vacuum for 4 hours to remove adsorbed moisture and gases. The bulk density was determined according to the WHO tapped density procedure (WHO, 2012) by measuring the volume occupied by 5 g of biosorbent in a 100 mL graduated cylinder after 10 tapping cycles.

2.4. Preparation of Synthetic Wastewater

Synthetic wastewater containing Ni(II), Cu(II), and Zn(II) ions was prepared by dissolving predetermined quantities of NiSO4.6H2O, CuSO4.5H2O, and ZnCl2 in deionized water. Three stock solution concentrations were prepared: 10 g/L, 20 g/L, and 30 g/L total metal content, representing low, medium, and high contamination scenarios encountered in

typical industrial effluents. Working solutions were obtained by appropriate dilution of stock solutions with deionized water. The pH, total dissolved solids (TDS), dissolved oxygen (DO), chemical oxygen demand (COD), and biological oxygen demand (BOD) of each solution were measured prior to adsorption experiments using standard analytical methods (APHA, 2017). Metal ion concentrations were verified using Atomic Absorption Spectrophotometry (AAS) at characteristic wavelengths for each metal.

2.5. Fixed-Bed Column Adsorption System

The continuous adsorption experiments were conducted in a laboratory-scale fixed-bed column system fabricated from transparent acrylic tubing with an internal diameter of 2.5 cm and total length of 50 cm. The column was equipped with detachable Teflon end caps, inlet and outlet ports, and a MEDO XG6 solenoid dosing pump for precise flow control. Glass wool (5 mm thickness) was placed at both ends of the column to prevent adsorbent loss and ensure uniform flow distribution. A 5 cm layer of glass beads (5 mm diameter) was positioned at the column base to support the biosorbent bed and promote uniform influent distribution. The nitric acid-treated L. cylindrica seeds were packed in the column between the glass wool layers to achieve the desired bed heights of 5 cm, 7.5 cm, and 10 cm, corresponding to biosorbent masses of approximately 5 g, 7.5 g, and 10 g, respectively. The packed bed was conditioned by passing deionized water upward through the column for 30 minutes to remove entrapped air bubbles and ensure complete wetting of the biosorbent. The synthetic metal solution was then pumped into the column at predetermined flow rates of 5, 10, and 15 mL/min using the calibrated dosing pump. Effluent samples were collected at regular time intervals and analyzed for residual metal concentrations and physicochemical parameters. All experiments were conducted at ambient temperature (29 plus or minus 2 degrees C) and performed in duplicate to ensure reproducibility.

2.6. Analytical Methods

The concentrations of Ni(II), Cu(II), and Zn(II) ions in the effluent samples were determined using a Buck Scientific Atomic Absorption Spectrophotometer (Model 210VGP) equipped with hollow cathode lamps for each metal. Calibration curves were prepared using certified standard solutions (1000 mg/L) with correlation coefficients exceeding 0.999. The pH was measured using a Benchtop pH meter (Model B200E, INFITEK India) calibrated with pH 4.0, 7.0, and 10.0 standard buffer solutions. Total dissolved solids (TDS) and electrical conductivity (EC) were measured using a digital conductivity meter (Hanna HI 9033). Dissolved oxygen (DO) was determined by the Winkler titrimetric method. Chemical oxygen demand (COD) was analyzed by the closed reflux dichromate method using a COD digester (Hach DRB 200), and biological oxygen demand (BOD5) was determined by the 5-day incubation method at 20 degrees C (APHA, 2017). The percentage removal efficiency (R%) for each metal was calculated using Equation (1):

$$R\% = [(C0 - Ct) / C0] \times 100\% \quad (1)$$

where C0 represents the initial metal concentration (mg/L) and Ct denotes the effluent metal concentration at time t (mg/L). The equilibrium adsorption capacity qe (mg/g) was calculated using Equation (2):

$$qe = (C0 - Ce) \times V / m \quad (2)$$

where Ce is the equilibrium concentration (mg/L), V is the solution volume (L), and m is the biosorbent mass (g).

3. Results and discussion

3.1. Characterization of *Luffa cylindrica* Seed Biosorbent

3.1.1. Physical Properties

The physical properties of the nitric acid-treated L. cylindrica seed biosorbent are summarized in Table 1. The BET surface area of 23.971 m squared/g, though relatively modest compared to commercial activated carbons (typically 500-1500 m squared/g), is consistent with values reported for other lignocellulosic biosorbents (Nwosu-Obieogu*et al*., 2020; Moreno-Rubio *et al*., 2025). The pore diameter of 2.402 nm classifies the material as mesoporous (2-50 nm), facilitating the diffusion of hydrated metal ions (typically 0.4-0.8 nm hydrated radius) into the pore structure. The total pore volume of 0.011 cc/g indicates limited internal porosity, suggesting that external surface adsorption may contribute significantly to the overall metal uptake. The bulk density of 0.34 g/cm cubed reflects the lightweight, fibrous nature of the seed material, which provides advantages for column packing and low pressure drop during operation.

Table 1 Physical Properties of L. Cylindrica Seed Biosorbent

Property	Value	Classification
BET Surface Area	23.971 m squared/g	Low surface area
Pore Volume	0.011 cc/g	Microporous-mesoporous
Pore Diameter	2.402 nm	Mesoporous (2-50 nm)
Bulk Density	0.34 g/cm cubed	Lightweight fibrous

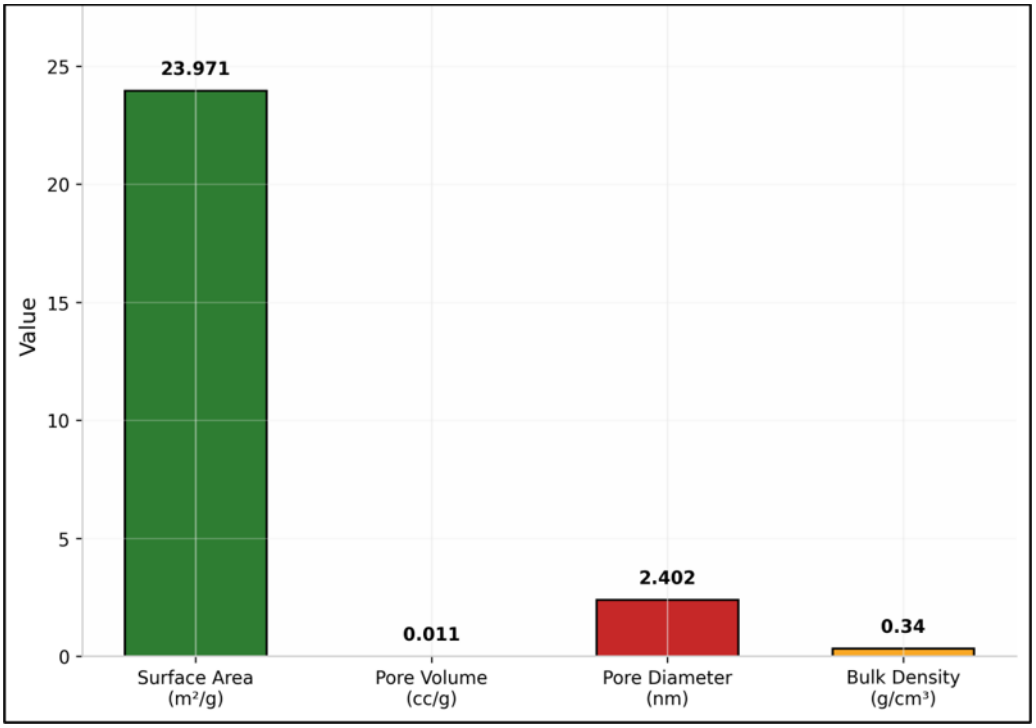

Figure 1 Physical properties of nitric acid-treated L. cylindrica seed biosorbent

3.1.2. Elemental Composition

The elemental composition determined by SEM-EDS analysis revealed carbon (73.13 wt.%) and nitrogen (21.41 wt.%) as the predominant elements, with minor contributions from potassium (1.39%), phosphorus (1.13%), magnesium (0.68%), sulfur (0.60%), silicon (0.50%), aluminum (0.41%), chlorine (0.30%), sodium (0.30%), and calcium (0.15%). The high carbon content reflects the lignocellulosic composition of the seed material, while the substantial nitrogen percentage suggests the presence of proteinaceous compounds and amino acid residues that may participate in metal coordination (Mazali& Alves, 2005). The oxygen-containing groups associated with the carbon framework provide the primary binding sites for metal chelation through ion exchange and complexation mechanisms.

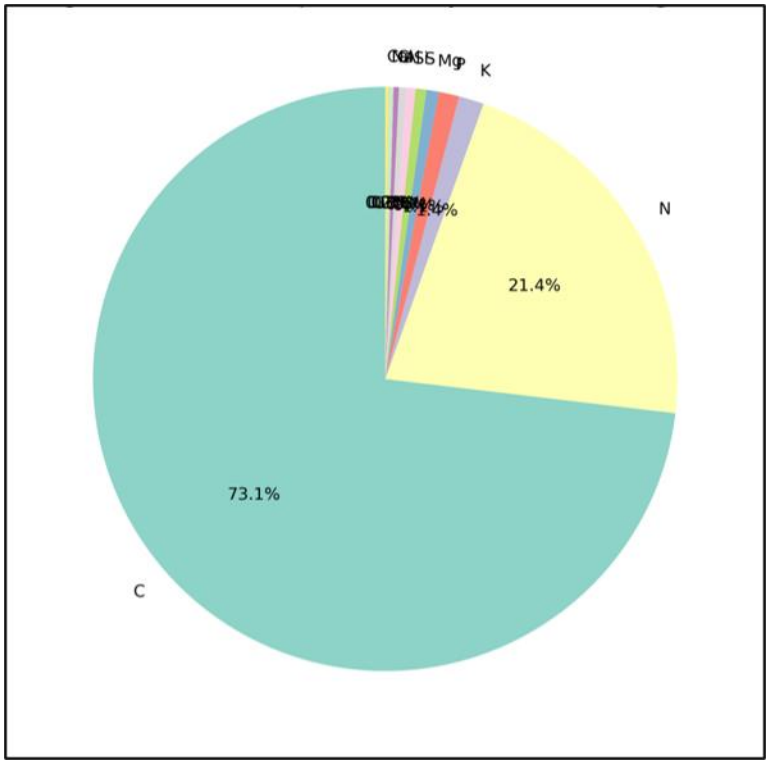

Figure 2 Elemental composition of L. cylindrica seeds (weight %)

3.1.3. FTIR Analysis

The FTIR spectra of raw and metal-loaded L. cylindrica seeds are presented in Figure 3. The broad and intense absorption band at 3280.1 cm-1 is attributed to O-H stretching vibrations arising from intermolecular and intramolecular hydrogen bonding in hydroxyl groups of cellulose, hemicellulose, and lignin (Eletta *et al*., 2019). The band at 3008.0 cm-1 corresponds to C-H stretching vibrations, while the peaks at 2922.2 cm-1 and 2847.7 cm-1 are associated with C-H asymmetric and symmetric stretching in aliphatic methylene groups. The absorption at 1543.2 cm-1 indicates C=C stretching in aromatic rings of lignin, and the prominent peak at 1032.5 cm-1 represents C-O stretching vibrations in alcohols, phenols, and carboxylic acids. Following metal adsorption, notable shifts in peak positions and intensities were observed, particularly in the O-H and C-O stretching regions, confirming the participation of these functional groups in metal binding through electrostatic attraction, ion exchange, and surface complexation mechanisms (Ullah *et al*., 2020).

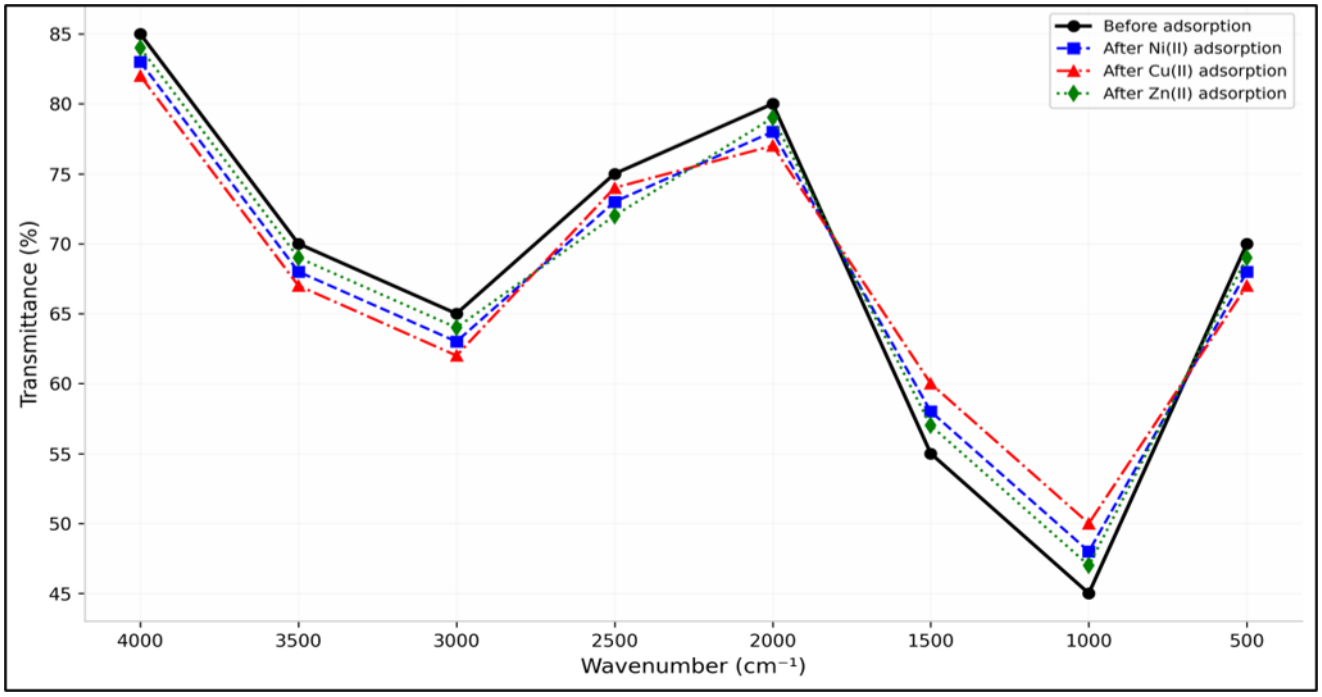

Figure 3 FTIR spectra of L. cylindrica seeds before and after metal adsorption

3.1.4. SEM Analysis

The SEM micrographs at magnifications of 500x, 1000x, and 2000x revealed the characteristic fibrous and macroporous structure of L. cylindrica seeds. The transverse sections displayed an interconnected network of fibers with visible fissures, cracks, and pores that provide accessible pathways for metal ion diffusion. The irregular surface morphology with heterogeneous texture offers abundant adsorption sites through edge effects and surface roughness. The macroporous structures observed at higher magnifications facilitate rapid mass transfer by allowing metal ions to penetrate deep into the biosorbent matrix. The relatively low surface area measured by BET analysis is attributed to the predominance of macropores that contribute minimally to nitrogen adsorption at 77 K, as opposed to micropores and small mesopores (Passos *et al*., 2006).

3.2. Effect of Bed Height on Adsorption Performance

The effect of bed height on the simultaneous removal of Ni(II), Cu(II), and Zn(II) ions was investigated at constant flow rate (5 mL/min) and particle size (75 micrometer) using three bed heights: 5 cm, 7.5 cm, and 10 cm. Figure 4 presents the pH variation of the effluent as a function of bed height for the three initial concentrations. The results demonstrate a progressive increase in effluent pH with increasing bed height for all concentrations. At 10 g/L initial concentration, the pH increased from 4.6 (untreated) to 5.3, 6.2, and 6.9 at bed heights of 5, 7.5, and 10 cm, respectively. Similarly, for 20 g/L and 30 g/L solutions, the pH showed corresponding improvements toward neutral values. This pH enhancement is attributed to the proton-consuming nature of the adsorption process, where H+ ions are exchanged from the biosorbent surface functional groups with metal cations from solution, effectively neutralizing the acidic wastewater (Bernal *et al*., 2017).

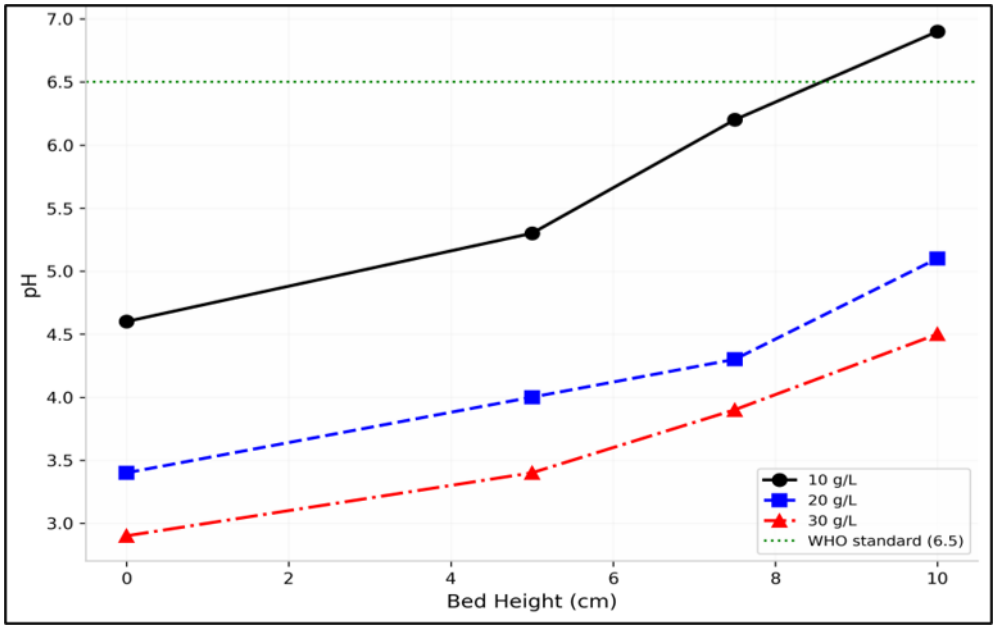

Figure 4 Effect of bed height on effluent pH (Q = 5 mL/min, particle size = 75 micrometer)

The metal removal efficiency exhibited a strong positive correlation with bed height, as illustrated in Figure 5. Increasing the bed height from 5 to 10 cm substantially enhanced removal efficiency for all three metal ions, with the maximum removal of 83.07% for Ni(II), 51.66% for Cu(II), and 55.73% for Zn(II) achieved at 10 cm bed height and 10 g/L initial concentration. The enhanced performance at greater bed heights can be attributed to several factors: increased availability of active binding sites proportional to biosorbent mass, extended contact time between metal ions and the adsorbent surface, and more effective utilization of the mass transfer zone (MTZ). The increasing bed depth provides a longer path for metal ions to interact with the biosorbent, facilitating greater opportunity for adsorption before breakthrough occurs (Saha *et al*., 2012).

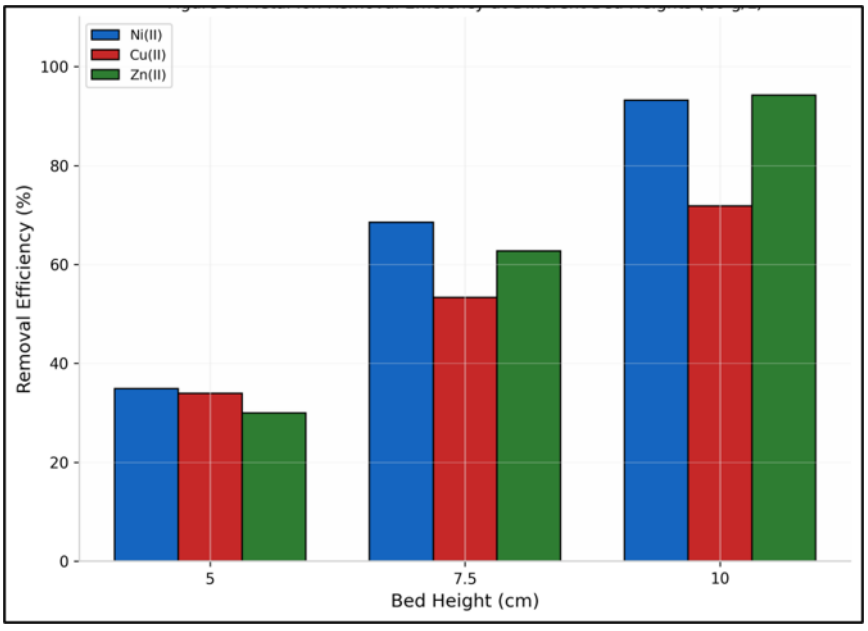

Figure 5 Metal removal efficiency at different bed heights (C0 = 10 g/L, Q = 5 mL/min)

3.3. Effect of Flow Rate on Adsorption Performance

The influence of injection flow rate on adsorption performance was evaluated at constant bed height (5 cm) and particle size (75 micrometer) using flow rates of 5, 10, and 15 mL/min. As depicted in Figure 6, the effluent pH decreased progressively with increasing flow rate across all initial concentrations. At 10 g/L, the pH declined from 5.3 at 5 mL/min

to 4.7 at 10 mL/min and further to 4.6 at 15 mL/min, approaching the untreated solution pH of 4.6. This trend indicates reduced adsorption efficiency at higher flow rates due to insufficient contact time for proton exchange reactions to proceed to equilibrium.

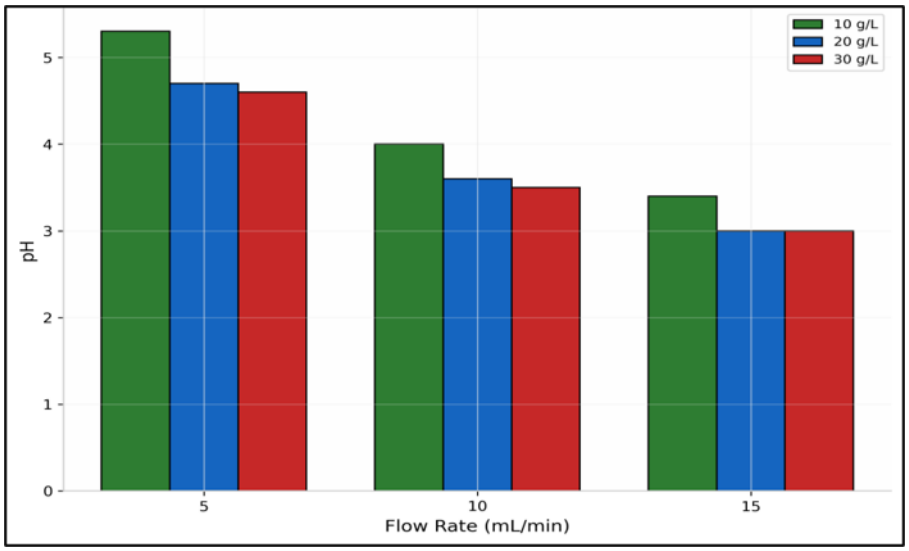

Figure 6 Effect of flow rate on effluent pH (Z = 5 cm, particle size = 75 micrometer)

The metal removal efficiency data presented in Figure 7 demonstrates an inverse relationship between flow rate and removal efficiency. At 10 g/L initial concentration, Ni(II) removal decreased from 34.9% at 5 mL/min to 26.9% at 10 mL/min and 23.4% at 15 mL/min. Similar declining trends were observed for Cu(II) and Zn(II) ions. The reduced performance at elevated flow rates is attributable to decreased hydraulic residence time within the packed bed, limiting the time available for metal ions to diffuse to active binding sites and establish equilibrium. Additionally, higher flow rates increase hydrodynamic shear forces at the biosorbent surface, potentially causing desorption of weakly bound metal ions and promoting channeling effects that bypass active adsorption zones (Cantel*iet al*., 2014).

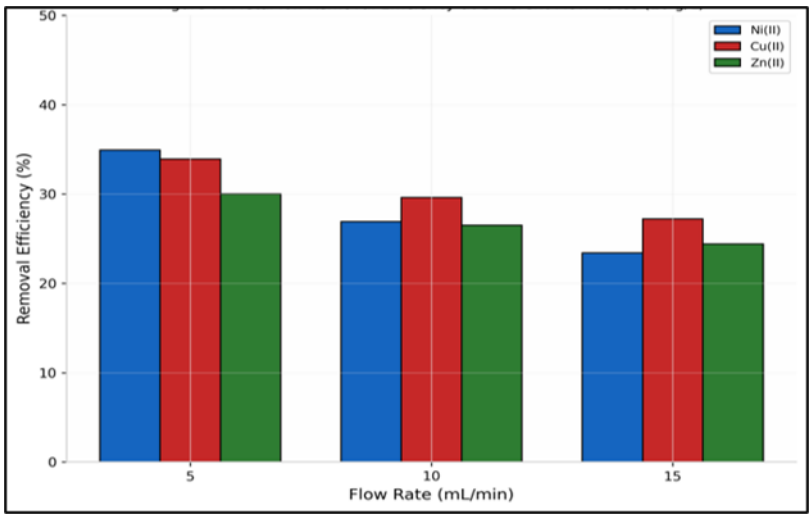

Figure 7 Metal removal efficiency at different flow rates (C0 = 10 g/L, Z = 5 cm)

3.4. Effect of Particle Size on Adsorption Performance

The effect of adsorbent particle size was investigated using three size fractions: 75 micrometer, 150 micrometer, and 300 micrometer at constant bed height (5 cm) and flow rate (5 mL/min). Figure 8 illustrates the TDS variation as a function of particle size. The TDS removal was most effective at the smallest particle size (75 micrometer), with values decreasing from 16,342 mg/L (untreated) to 14,704 mg/L, 15,753 mg/L, and 16,125 mg/L for 75, 150, and 300 micrometer particles, respectively, at 10 g/L initial concentration. The superior performance of smaller particles is

attributed to their larger external surface area-to-volume ratio, providing greater accessibility of binding sites and shorter intraparticle diffusion paths (Han *et al*., 2008).

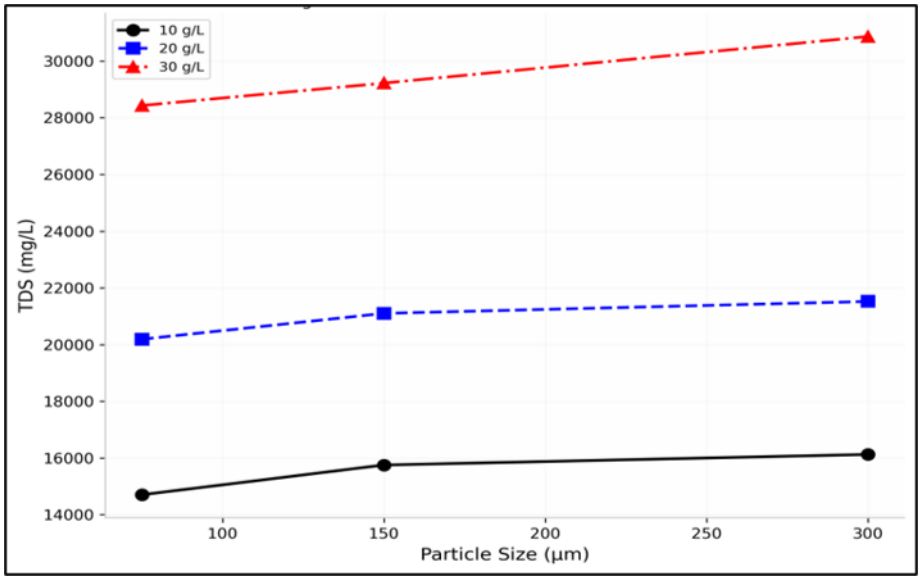

Figure 8 Effect of adsorbent particle size on TDS removal (Z = 5 cm, Q = 5 mL/min)

The metal removal efficiency data (Figure 9) confirms the inverse relationship between particle size and adsorption performance. At 10 g/L initial concentration, Ni(II) removal decreased from 34.9% at 75 micrometer to 26.7% at 150 micrometer and 5.6% at 300 micrometer. Similar trends were observed for Cu(II) and Zn(II), with the most dramatic decline occurring between 150 and 300 micrometer. Larger particles exhibit increased diffusion resistance within the porous matrix, reducing the effective utilization of internal binding sites. Furthermore, larger interparticle voids in beds packed with coarse particles promote preferential flow pathways that reduce contact efficiency between metal ions and the biosorbent surface.

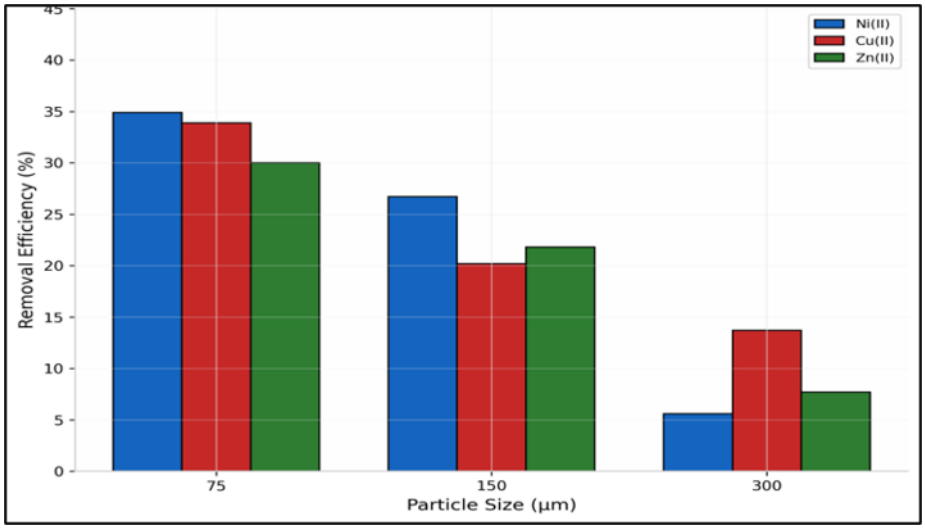

Figure 9 Metal removal efficiency at different particle sizes (C0 = 10 g/L, Z = 5 cm, Q = 5 mL/min)

3.5. 3.5 Effect on Physicochemical Parameters

The comprehensive effects of operational parameters on key physicochemical indicators are presented in Figure 10. COD and BOD removal demonstrated consistent patterns across all parameter variations, with maximum reductions achieved at optimal conditions (10 cm bed height, 5 mL/min flow rate, 75 micrometer particle size). The COD decreased by up to 89.6% (from 11,757 to 1,218 mg/L at 10 g/L, 10 cm height), while BOD reduction reached 90.8% (from 6,778 to 623 mg/L). The dissolved oxygen (DO) content showed marked improvement from 0.063 mg/L (untreated) to 1.891

mg/L at optimal conditions, reflecting the substantial reduction in oxygen-demanding pollutants. These improvements in physicochemical parameters demonstrate that the L. cylindrica biosorbent system simultaneously addresses multiple water quality indicators beyond heavy metal removal.

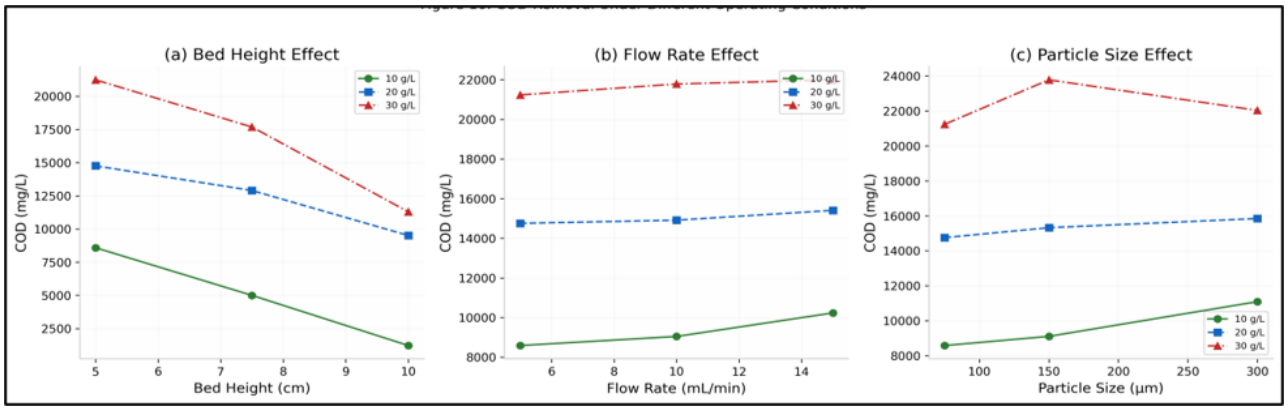

Figure 10 COD removal under different operating conditions: (a) bed height effect, (b) flow rate effect, (c) particle size effect

Table 2 Physicochemical and Metal Removal Efficiency of L. Cylindrica Seed Biosorbent at Different Bed Heights

Parameter	Untreated (10 g/L)	5 cm	7.5 cm	10 cm	% Removal at 10 cm
pH	4.6	5.3	6.2	6.9	50.0
TDS (mg/L)	16,342	14,704	12,921	6,705	59.0
DO (mg/L)	0.063	0.168	0.903	1.891	2899.7
COD (mg/L)	11,757	8,586	4,996	1,218	89.6
BOD (mg/L)	6,778	4,535	2,034	623	90.8
Ni(II) (mg/L)	943	614	297	64	93.2
Cu(II) (mg/L)	1,543	1,020	721	435	71.8
Zn(II) (mg/L)	1,334	934	498	78	94.2

3.6. Adsorption Selectivity and Mechanism

The comparative analysis of metal removal efficiencies revealed distinct adsorption affinities following the order Ni(II) >Zn(II) >Cu(II) under most operating conditions. This selectivity sequence may be attributed to the combined influence of ionic radii, electronegativity, hydration enthalpy, and the formation constants of metal-ligand complexes with the biosorbent surface functional groups. Ni(II) ions exhibit favorable adsorption characteristics due to their smaller hydrated radius and higher charge density, facilitating stronger electrostatic interactions with the negatively charged biosorbent surface at near-neutral pH conditions (Kuyucak& Volesky, 1989). The observed shifts in FTIR spectra following metal loading, particularly the intensity changes in O-H and C-O stretching bands, confirm that the primary adsorption mechanisms involve ion exchange between protons from carboxyl and hydroxyl groups with metal cations, complemented by surface complexation and electrostatic attraction (Volesky, 2003). The exothermic nature of the adsorption process and the dominance of chemisorption are evidenced by the excellent fit of the pseudo-second-order kinetic model (R squared = 1.000), which describes adsorption processes where electron sharing or transfer occurs between the adsorbate and adsorbent.

4. Conclusion

This study successfully demonstrated the effectiveness of nitric acid-treated *Luffa cylindrica* seeds as a sustainable, low-cost biosorbent for the simultaneous removal of Ni(II), Cu(II), and Zn(II) ions from aqueous solutions in a continuous fixed-bed column system. The comprehensive characterization revealed a mesoporous lignocellulosic material with abundant oxygen-containing functional groups capable of binding heavy metal ions through multiple mechanisms. The

parametric optimization studies established that bed height exerts the most significant positive influence on removal efficiency, followed by particle size and flow rate as inverse factors. Maximum removal efficiencies of 83.07% for Ni(II), 51.66% for Cu(II), and 55.73% for Zn(II) were achieved at optimal conditions of 10 cm bed height, 5 mL/min flow rate, and 75 micrometer particle size. The biosorbent simultaneously improved multiple water quality indicators, achieving COD and BOD reductions exceeding 89% and DO restoration to environmentally acceptable levels. The chemisorption-dominated mechanism, validated by the pseudo-second-order kinetic model, ensures stable metal binding resistant to desorption under moderate hydraulic conditions. These findings establish L. cylindrica seeds as a promising locally sourced alternative to commercial activated carbon for heavy metal remediation, contributing to both environmental sustainability and agricultural waste valorization in developing tropical economies. Future studies should investigate regeneration and reusability protocols, competitive adsorption in multi-component systems, and scale-up to pilot-scale continuous treatment plants.

Compliance with ethical standards

Acknowledgments

The authors wish to thank the management and technical staff of the department of Chemical/Petrochemical Engineering, Rivers State University, for granting the authors access to their laboratories.

Disclosure of conflict of interest

No conflict of interest to be disclosed.

References

[1] Abdel-Ghani, N. T., Hefny, M., & El-Chaghaby, G. A. F. (2009). Factorial experimental design for biosorption of iron and zinc using Typha domingensisphytomass. Desalination, 249, 343-347.

[2] Adeyinka, A., Liang, H., & Tina, G. (2007). Removal of metal ions from wastewater with natural waste materials. Journal of Environmental Engineering, 133(11), 1088-1093.

[3] Ariffin, N., Abdullah, M. M., Zainol, M. R., & Murshed, M. F. (2017). Review on adsorption of heavy metal in wastewater by using geopolymer. MATEC Web of Conferences, 97, 01023.

[4] Babel, S., & Kurniawan, T. A. (2003). Low-cost adsorbents for heavy metals uptake from contaminated water: A review. Journal of Hazardous Materials, 97(1-3), 219-243.

[5] Bernal, V., Erto, A., Giraldo, L., & Moreno-Pirajan, J. (2017). Effect of solution pH on the adsorption of paracetamol on chemically modified activated carbons. Molecules, 22(7), 1-14.

[6] Canteli, A. M. D., Carpine, D., Scheer, A. P., Mafra, M. R., & Igarashi-Mafra, L. (2014). Fixed-bed column adsorption of the coffee aroma compound benzaldehyde from aqueous solution onto granular activated carbon from coconut husk. LWT-Food Science and Technology, 59, 1025-1032.

[7] Chen, J. D., Yu, J. X., Wang, F., Tang, J. Q., Zhang, Y. F., & Chi, R. A. (2017). Selective adsorption and recycle of Cu2+ from aqueous solution by modified sugarcane bagasse under dynamic condition. Environmental Science and Pollution Research, 24, 1-8.

[8] Dabrowski, A. (2001). Adsorption - from theory to practice. Advances in Colloid and Interface Science, 93, 135-224.

[9] Eletta, O., Adewoye, L., Mustapha, S., Adeniyi, A., & Ogunleye, O. (2019). Modelling and optimization of oil extraction from Loofah (*Luffa cylindrica*) seeds using a binary solvent mixture. Journal of the Turkish Chemical Society, 2, 57-68.

[10] Gupta, N., Prasad, M., Singhal, N., & Kumar, V. (2009). Modeling the adsorption kinetics of divalent metal ions onto pyrophyllite. Industrial & Engineering Chemistry Research, 48(4), 2125-2128.

[11] Gupta, V. K., & Ali, I. (2013). Water treatment for inorganic pollution by adsorption technology. In Environmental Water (pp. 29-91). Springer.

[12] Han, B., Miranda, C., & Ceder, G. (2008). Effect of particle size and surface structure on adsorption of O and OH-on platinum nanoparticles. Physical Review B, 77, 1-9.

[13] Himanshu, P. (2019). Fixed-bed column adsorption study: A comprehensive review. Applied Water Science, 9, 45-62.

[14] Kuyucak, N., & Volesky, B. (1989). Accumulation of cobalt by marine alga. Biotechnology and Bioengineering, 33(7), 809-814.

[15] Laidani, E. A., Zine, B., Benabed, B., & Kadri, E. H. (2020). Experimental investigation on effects of calcined bentonite on fresh, strength and durability properties. Construction and Building Materials, 230, 117062.

[16] Mazali, I. O., & Alves, O. L. (2005). Morphosynthesis: High fidelity inorganic replica of the fibrous network of loofa sponge (*Luffa cylindrica*). Anais da Academia Brasileira de Ciencias, 77 (1), 25-31.

[17] Moreno-Rubio, J. G., Osornio-Rubio, N. R., Jimenez-Islas, H., & Martinez-Gonzalez, G. M. (2025). Characterization and efficiency of *Luffa cylindrica* as bioadsorbent in Cr(VI) removal from synthetic wastewater. Environmental Technology & Innovation, 33, 103562.

[18] Nwosu-Obieogu, K., Dzarma, G., Okolo, B. I., &Akatobi, K. (2020). Adsorption of vanadium(V) from textile industry effluent using *Luffa cylindrica* activated carbon. Journal of Chemistry and Chemical Engineering, 14, 129-135.

[19] Ojong, E. O. & Wosu, C. O. (2025). Production and characterization of adsorbents from corncorbs for removal of hexavalent chromium ions from tannery effluent. Irish International Journal of Engineering and Scientific Studies, 8 (4), 1 – 35.

[20] Ojong, E. O., Benibo, P. D. & Wosu, C. O. (2025). Design and optimization of CO2 capture process from stream of gas mixture at elevated temperature using composites of nanoparticles. Advance Journal Science, Engineering and Technology, 10 (8), 1 – 20.

[21] Okezua, C. A., Ojong, E. O. & Wosu, C. O. (2025). The synthesis of activated carbon from gmelina trunk. International Journal of Engineering Research Updates, 8 (1), 8 – 16. https://doi.org/10.53430/ijeru.2025.8.1.0024.

[22] Passos, C. G., Lima, E. C., Arenas, L. T., Simon, N. M., &Brasil, J. L. (2006). Use of statistical design of experiments to evaluate the sorption capacity. Journal of Colloid and Interface Science, 302, 396-407.

[23] Rakesh, N., Kalpana, P., Naidu, T. V. R., & Venkateswara Rao, M. (2010). Removal of zinc ions from aqueous solution by Ficus benghalensis L. International Journal of Engineering Studies, 2(1), 15-28.

[24] Richard, J. (2009). Adsorption of heavy metals from wastewater using low-cost materials. Journal of Environmental Management, 91(5), 1131-1137.

[25] Saha, P. D., Chakraborty, S., & Chowdhury, S. (2012). Batch and continuous (fixed-bed column) biosorption of crystal violet by Artocarpus heterophyllus leaf powder. Colloids and Surfaces B, 92, 262-270.

[26] Sasan, N. Z., Rafiee, R., &Jalilnejad, E. (2023). Experimental study on evaluation and optimization of heavy metals adsorption on a novel amidoximated silane functionalized *Luffa cylindrica*. Scientific Reports, 13 (1), 3670.

[27] Segun, E. O., Nurudeen, A. O., & Olumuyiwa, A. O. (2014). Adsorption of Brilliant Green onto *Luffa cylindrica* sponge: Equilibrium, kinetics, and thermodynamic studies. ISRN Environmental Chemistry, 2014, 743532.

[28] Singh, S. (2008). Adsorption behavior of Ni(II) from water onto zeolite X: Kinetics and equilibrium studies. Proceedings of World Congress on Engineering and Computer Science, 22-24.

[29] Tumin, N. D., Chuah, A. L., Zawani, Z., & Abdul Rashid, S. (2008). Adsorption of copper from aqueous solution by Elaeis guineensis kernel activated carbon. Journal of Engineering Science and Technology, 3(2), 180-189.

[30] Udeagbara, S. G., Okorodudu, E. A., Isehunwa, S. O., & Adeyi, A. A. (2025). Treatment of produced water from Niger Delta oilfields using chemically modified sponge gourd (*Luffa cylindrica*). Journal of Petroleum and Gas Engineering, 17(1), 1-13.

[31] Ullah, M., Nazir, R., Khan, M., Khan, W., & Afridi, S. G. (2020). The effective removal of heavy metals from water by activated carbon adsorbents. Soil and Water Research, 15, 30-37.

[32] Volesky, B. (2003). Sorption and biosorption. BV Sorbex Inc.

[33] Volesky, B., & Naja, G. (2007). Biosorption technology: Starting up an enterprise. International Journal of Technology Transfer and Commercialization, 6(2/3/4), 196-211.

[34] WHO. (2012). Bulk density and tapped density of powders. WHO Document QAS/11.450.

[35] WHO. (2017). Guidelines for drinking-water quality (4th ed.). World Health Organization.

[36] Wosu, C. O. (2024). Design of a CSTR to produce 2,000,000 tons per year of magnesium chloride from the neutralization reaction of magnesium oxide and hydrochloric acid. International Journal of Scientific and Research Publications, 14 (6), 528 – 548. https://doi.org/10.29322/IJSRP.14.06.2023.p15046.

[37] Wosu, C. O. & Ekokoye, A. B. (2025). Application of CSTR design thickness models for optimum production of magnesium chloride from neutralization reaction of magnesium oxide and hydrochloric acid. International Journal of Advanced Engineering and Technology, 9 (1), 1 – 8.